Phase estimation in driven discrete-time quantum walks

Shivani Singh,* Craig S. Hamilton,† and Igor Jex‡
FNSPE, Czech Technical University in Prague, Brêhová 7, 119 15 Praha 1, Czech Republic

(Received 27 June 2023; accepted 25 September 2023; published 12 October 2023)

Quantum walks have been shown to be important for quantum metrological tasks, in particular for the estimation of the evolution parameters of the walk. In this work, we address the enhancement of this parameter estimation using the driven discrete-time quantum walk (DDTQW), which is a variant of the discrete-time quantum walk with multiple walkers. DDTQW has two regimes based on the interference between the walker number, i.e., phase matched and phase mismatched. We derive an expression for the quantum Fisher information (QFI) in the phase-matched regime of DDTQW driven using the squeezing operator, demonstrating an exponential increase in QFI. In the phase-mismatched regime, QFI varies as t^2, consistent with previous studies. Our analysis shows that parameter estimation can be improved by driving the walk using squeezing operators.

DOI: 10.1103/PhysRevA.108.042607

I. INTRODUCTION

Quantum walks (QWs) are the subject of numerous studies in the field of quantum information processing applications [1–3]. Theoretically, QWs have been shown to be universal for quantum computation [4–6] and have been used in various search algorithms [7,8]. They are also a popular tool for quantum simulations, e.g., photosynthesis [9], Anderson localization [10–12], Dirac cellular automata [13–15], neutrino oscillation [16], topological phenomena [17–19], and many more [20,21]. Experimentally, they have been implemented on various physical systems such as nuclear magnetic resonance (NMR) [22], photonics [23–25], trapped ions [26–28], and waveguide arrays [29,30]. They are the quantum analog of classical random walks (CRWs) [31–33], where the quantum walker can be in a superposition of position states on the defined spatial network of sites. One of the most common features of QWs is that they can spread faster than CRWs in space due to interference phenomena of the walker.

A QW has two main forms: continuous-time quantum walk (CTQW) and discrete-time quantum walk (DTQW) [34–38]. CTQW is described on a position Hilbert space and by a Hamiltonian that generally represents a graph topology (of edges and vertices) that the walker can move on. DTQW is defined on combined Hilbert spaces, i.e., the position and coin space (internal degree of freedom) of the walker. The latter variant usually evolves iteratively, first by applying a unitary coin operator that "flips" the coin state, and then a conditional shift operator that moves the walker in position space, dependent upon its coin state. The dynamics of the walk are generally controlled by the coin operation, which, for a one-dimensional (1D) walk with two internal coin states, is represented by an SU(2) operator [39], with three independent parameters.

The driven discrete-time quantum walk (DDTQW) [40,41] is a variation of DTQW, motivated by the experimental realizations of photonic QWs in waveguide arrays with a nonlinear down-conversion process and optical delay loops pumped with laser light [42–44]. In DDTQW, walkers can be coherently created and destroyed at each time step of the walk, possibly interfering with walkers already present in the system. This is represented by the addition of extra terms in the iterative evolution, which in previous studies were either displacement or squeezing operators, representing the pumping by coherent and squeezed light, respectively. It was shown that DDTQW can have very different dynamics than the original DTQW, primarily due to phase-matching conditions between the pumped terms and eigenmodes of the system.

Parameter estimation has applications in various fields of modern science, e.g., gravitational wave detection, microscopy and imaging, Hamiltonian estimation, and general sensing technologies [45–48]. The measurement uncertainty can be characterized by the quantum Cramer-Rao bound, which gives a bound over precision of the estimated parameter in terms of quantum Fisher information (QFI) [49], which a detection scheme would seek to maximize. Typically, interferometric methods are used to measure the parameter, which is encoded in the path difference of the interferometer. Quantum walks (QWs) can be considered as a multipath interferometer [50], and their use for parameter estimation has been explored in the past [51–53]. Here we are improving the parameter estimation by maximizing the QFI using a variant of the QW using squeezed state driving.

Quantum metrological schemes have been proposed in the past and precision benchmarks have been obtained for both CTQWs [51] and DTQWs [52,53], where in the latter they estimate the phase parameter of the SU(2) operator representing the coin. There it was shown that the QFI for the SU(2)-parameter estimation increases quadratically with

*singhshi@fjfi.cvut.cz
†hamilcra@fjfi.cvut.cz
‡igor.jex@fjfi.cvut.cz

the number of steps, t, i.e., as t^2. In this work, we are proposing a protocol to improve the precision of phase estimation in the SU(2) operator using DDTQW.

The paper is organized as follows. Section II gives an analytical introduction to DDTQW, which is driven using squeezing operators. Section III presents our main results and shows the analytical and numerical calculations of QFI for the two different regimes of DDTQW, i.e., phase matched and phase mismatched. We also compare our phase estimation method with previous approaches. In Sec. IV, we present a bound over the pump phase to achieve enhanced precision. Section V concludes our results with a discussion.

II. DRIVEN DISCRETE-TIME QUANTUM WALK

The DDTQW is a variant of QWs where there is either coherent or squeezed driving of the walker number at each step of the walk. This can result in walkers being added throughout the walk, instead of only at the beginning in the initial state [41]. We start by describing the dynamics of the original, passive DTQW in the physical basis and focus on the graph structure of a cyclic graph with periodic boundary conditions.

A. Dynamics of discrete-time quantum walk

A one-dimensional DTQW with a single walker in the physical basis is defined on a Hilbert space $\mathcal{H} = \mathcal{H}_p \otimes \mathcal{H}_c$, where $\mathcal{H}_c$ is the coin Hilbert space spanned by the internal degree of freedom of the walker $\{|L\rangle, |R\rangle\}$, and $\mathcal{H}_p$ is the position Hilbert space spanned by $\{|x \mod N\rangle, x \in N\}$, where N is the number of sites on the underlying graph structure that the walker can travel on.

The walker evolves by applying the coin operation C, followed by a conditional shift operation S. The general form of the coin operator is a SU(2) operator, given by

$$C(\theta, \xi, \zeta) = \sum_{x=1}^{N} |x\rangle\langle x| \otimes \begin{pmatrix} e^{i\xi}\cos\theta & e^{i\zeta}\sin\theta \\ -e^{-i\zeta}\sin\theta & e^{-i\xi}\cos\theta \end{pmatrix}. \quad (1)$$

The topology of the graph defines the shift operation and it is defined by the sites which are coupled. On a cyclic graph of N sites, the shift operator is

$$S = \sum_{x=1}^{N} (|x-1 \mod N\rangle\langle x| \otimes |L\rangle\langle L| + |x+1 \mod N\rangle\langle x| \otimes |R\rangle\langle R|). \quad (2)$$

Thus the walker's wave function $|\Psi(t+1)\rangle$ after $(t+1)$ steps is described as

$$|\Psi(t+1)\rangle = SC(\theta, \xi, \zeta)|\Psi(t)\rangle = U|\Psi(t)\rangle. \quad (3)$$

In general, $|\Psi(t+1)\rangle$ can also be represented as

$$|\Psi(t+1)\rangle = \sum_x |x\rangle[\psi_L(x, t+1)|L\rangle + \psi_R(x, t+1)|R\rangle], \quad (4)$$

where $\psi_L(x)$ is the probability amplitude associated with $|L\rangle$ and $\psi_R(x)$ is the probability amplitude associated with $|R\rangle$, such that it can be represented by a two-component vector $\tilde{\Psi}(x) = [\psi_L(x), \psi_R(x)]^T$ at position x, where

$$\tilde{\Psi}(x, t+1) = \begin{pmatrix} e^{i\xi}\cos\theta & e^{i\zeta}\sin\theta \\ 0 & 0 \end{pmatrix}\tilde{\Psi}(x+1, t) + \begin{pmatrix} 0 & 0 \\ -e^{-i\zeta}\sin\theta & e^{-i\xi}\cos\theta \end{pmatrix}\tilde{\Psi}(x-1, t). \quad (5)$$

The analytical analysis of the DDTQW is simplified by transforming the dynamics from the physical basis to the eigenbasis of the evolution operation, U. To obtain the eigenvalues and eigenbasis of this operator, we first transform the state of the walker from the position basis $|x\rangle$ to the momentum basis $|k\rangle$ using the Fourier transformation. After the Fourier transformation, the evolution operator is diagonal in the position Hilbert space.

Basis transformation to the Fourier space. In Fourier space, the probability amplitude $\tilde{\Psi}(x)$ transforms to $\tilde{\Psi}(k) = [\psi_L(k), \psi_R(k)]^T$, a two-component wave function, and k are the wave vectors. The transformation to Fourier space on the cyclic graph of N sites is given by

$$\tilde{\Psi}(k) = \frac{1}{\sqrt{N}} \sum_x e^{i2\pi k.x/N}\tilde{\Psi}(x). \quad (6)$$

Substituting this in Eq. (5) will give the wave function in the Fourier space such that

$$|\Psi(k, t+1)\rangle = U_k|\Psi(k, t)\rangle, \quad (7)$$

where

$$U_k = \begin{pmatrix} e^{i(\xi-2\pi k/N)}\cos\theta & e^{i(\zeta-2\pi k/N)}\sin\theta \\ -e^{-i(\zeta-2\pi k/N)}\sin\theta & e^{-i(\xi-2\pi k/N)}\cos\theta \end{pmatrix}, \quad (8)$$

for each wave vector $k \in [1, N]$. The transformation matrix T_f from the physical basis to the Fourier basis has the matrix elements given by $(T_f)_{k,x} = e^{i2\pi k.x/N}$.

Basis transformation to the eigenspace of U. An analytical expression for the eigenbasis and eigenvalues of the operator U can be obtained by diagonalizing U_k, given by Eq. (8), for each k, such that the evolution operator in the eigenbasis is

$$U_{\text{eig}} = \sum_{j=1}^{2N} E_j = \bigoplus_{k=1}^{N} (T_E U_k T_E^\dagger), \quad (9)$$

where $\{E_j\}$ are the set of eigenoperators. T_E is the transformation matrix that takes the state from the Fourier basis to eigenbasis and is given by

$$T_E = \bigoplus_{k=1}^{N} \begin{pmatrix} -e^{i(\zeta-\frac{2\pi k}{N})}\sin\theta & e^{-i(\xi-\frac{2\pi k}{N})}\cos\theta - e^{i\Omega_k} \\ e^{i(\xi-\frac{2\pi k}{N})}\cos\theta - e^{-i\Omega_k} & e^{-i(\zeta-\frac{2\pi k}{N})}\sin\theta \end{pmatrix}. \quad (10)$$

The evolution operator in the eigenbasis is

$$U_{\text{eig}} = \bigoplus_{k=1}^{N} \begin{pmatrix} e^{-i\Omega_k} & 0 \\ 0 & e^{i\Omega_k} \end{pmatrix} = \sum_{m=1}^{2N} e^{-i\Omega_m \hat{A}_m^\dagger \hat{A}_m}, \quad (11)$$

where $\{e^{i\Omega_m}\}$ are the eigenvalues of U_{eig} and Ω_m are termed eigenfrequencies. The eigenfrequencies $\{\Omega_m\} = \{\pm\Omega_k\}$ in terms of wave vector k are determined by the dispersion relation [55],

$$\cos\Omega_k = \cos\left(\frac{2\pi k}{N} - \xi\right)\cos\theta. \tag{12}$$

The bosonic operators in the eigenbasis are transformed as $\hat{A}_l^\dagger = \sum_{j=1}^{2N}(T_{\text{eig}})_{l,j}\hat{a}_j^\dagger$, where $T_{\text{eig}} = T_E \cdot T_f$ is the transformation matrix from the physical basis to the eigenbasis.

B. Dynamics of driven discrete-time quantum walk

In this work, we assume the walkers to be indistinguishable bosons, and thus our Hilbert space expands to include their number space $\mathcal{H}_{DDTQW} = \mathcal{H}_{DTQW} \otimes \mathcal{H}_n$. To model the walkers, we use bosonic annihilation and creation operators such that $\hat{a}_{x,c}^\dagger(\hat{a}_{x,c})$ are the creation (annihilation) operators for a photon (walker) with coin state c at position x [also referred to as the mode (x, c)]. Previous studies used squeezing and displacement operators in DDTQW, which have Hamiltonian terms $\hat{a}^{\dagger 2}$ and $\hat{a}^\dagger$, respectively, which in general do not conserve the walker number [40,41]. In this work, we focus on using squeezing operators.

The general, multimode squeezing operator is

$$Sq(\Gamma) = \exp\left(\frac{1}{2}\sum_{i,j}\Gamma_{i,j}\hat{a}_i^\dagger\hat{a}_j^\dagger - \text{H.c.}\right), \tag{13}$$

where $\Gamma_{i,j}$ is the pump amplitude for the ith and jth modes. The single-mode squeezing operator is a special case of this,

$$Sq_1(\Gamma) = \exp\left(\frac{\Gamma}{2}\hat{a}_m^{\dagger 2} - \frac{\Gamma^*}{2}\hat{a}_m^2\right), \tag{14}$$

and the two-mode squeezing operator in the modes m and n is

$$Sq_2(\Gamma) = \exp(\Gamma\hat{a}_m^\dagger\hat{a}_n^\dagger - \Gamma^*\hat{a}_m\hat{a}_n). \tag{15}$$

The DDTQW evolves iteratively, as for the DTQW, but now with the inclusion of the squeezing operator at each time step. The evolution operator for the DDTQW using the squeezing operator after t steps is

$$\begin{aligned}|\Psi(t+1)\rangle &= SC(\theta,\xi,\zeta)Sq(\Gamma_t)|\Psi(t)\rangle \\ &= W|\Psi(t)\rangle = W^{(t+1)}|\Psi(0)\rangle,\end{aligned} \tag{16}$$

where $SC(\theta,\xi,\zeta)$ is the unitary operator given by the original DTQW, given by Eq. (3), and the squeezing operator is defined by a time-dependent pump shape Γ_t. The dynamics are best solved in the eigenbasis, where the evolution operation after t steps is given by

$$\prod_{j=1}^{t} W_{\text{eig}}|0\rangle = \prod_{j=1}^{t}[U_{\text{eig}}Sq(\Gamma_{\text{eig}})]|0\rangle, \tag{17}$$

where the pump shape of the squeezing operator is transformed to $\Gamma_{\text{eig}} = T_{\text{eig}}^{-1}\Gamma_t T_{\text{eig}}$ and U_{eig} is a simple phase term, (11).

When the squeezing operators that are used are either the single- or two-mode operators, we can reorder the above equation using the simple relation [56]

$$Sq(\Gamma_{\text{eig}})e^{-i\hat{A}^\dagger\Omega\hat{A}} = e^{-i\hat{A}^\dagger\Omega\hat{A}}Sq(e^{\bar{i}\Omega}\Gamma_{\text{eig}}e^{i\Omega}), \tag{18}$$

where $e^{\bar{i}\Omega}$ is the transpose of the matrix $e^{i\Omega}$. This allows all the squeezing operators to be moved to the right of the QW operator, U_{eig}, which we will use in the next section. The overall pump amplitude $Sq(\Gamma_F)$ after t steps can be given by

$$\begin{aligned}Sq(\Gamma_F) = Sq(e^{i(t^{\bar{}}-1)\Omega}\Gamma_{\text{eig}}e^{i(t-1)\Omega})Sq(e^{i(t^{\bar{}}-2)\Omega}\Gamma_{\text{eig}}e^{i(t-2)\Omega}) \\ \times\cdots\times Sq(e^{\bar{i}\Omega}\Gamma_{\text{eig}}e^{i\Omega})Sq(\Gamma_{\text{eig}}),\end{aligned} \tag{19}$$

so that (17) can be written as

$$\prod_{j=1}^{t}[U_{\text{eig}}Sq(\Gamma_{\text{eig}})]|0\rangle = U_{\text{eig}}^t Sq(\Gamma_F)|0\rangle. \tag{20}$$

If the time dependence of Γ_{eig} is such that it counteracts the phase acquired from the reordering of U_{eig} through the squeezing operator in Eq. (17), then all the $Sq(\cdot)$ in (19) are identical and we have constructive interference between the operators. This is termed the phase-matched regime, with the alternative being the phase-mismatched regime. Here we have analyzed the dynamics of DDTQW in the phase-matched regimes, which is achieved when the pump frequency is equal to either twice a single eigenfrequency (single-mode case) or the sum of a pair of eigenfrequencies (two-mode case). This will lead to the final, overall squeezing operation to be well approximated by either a single-mode or a two-mode squeezing operation, depending upon the pump frequency.

Analysis of DDTQW using single-mode squeezing operator in eigenbasis. A simplified case for the analytical analysis of the squeezed DDTQW is using the single-mode squeezing operation, given by Eq. (14), in the eigenbasis and in the phase-matched regime.

The squeezing operation is applied on the eigenmode m and using the relation (18), for the single-mode operator,

$$Sq_1(\Gamma_{\text{eig}})e^{-i\Omega_m\hat{A}_m^\dagger\hat{A}_m} = e^{-i\Omega_m\hat{A}_m^\dagger\hat{A}_m}Sq_1(e^{i2\Omega_m}\Gamma_{\text{eig}}). \tag{21}$$

In the phase-matched regime, the pump shape in the eigenbasis is given by $\Gamma_{\text{eig}} = re^{-2i\omega(t-1)}$, where $\omega = 2\Omega_m$, and thus the final squeezing operator, given by Eq. (19), is

$$\begin{aligned}Sq_1(\Gamma_F) &= Sq_1(r)Sq_1(r)Sq_1(r)\cdots Sq_1(r) \\ &= [Sq_1(r)]^t.\end{aligned} \tag{22}$$

The evolution operator in the eigenbasis of this case is

$$\begin{aligned}W_{\text{eig}}|0\rangle &= U_{\text{eig}}^t Sq_1(\Gamma_F)|0\rangle \\ &= U_{\text{eig}}^t(Sq_1(r))^t|0\rangle,\end{aligned} \tag{23}$$

where U_{eig} is the evolution operator in the eigenbasis given by Eq. (11). The covariance matrix for the vacuum state $|0\rangle$ is $\frac{1}{2}\mathcal{I}$, where $\mathcal{I}$ is the identity matrix.

The symplectic form of the squeezing operator $Sq_1(\Gamma_F)$ [57] when phase matched with the eigenmode $m = 1$ is

$$Sq_1(\Gamma_F) = \begin{pmatrix}\cosh(rt) & -\sinh(rt)\\ -\sinh(rt) & \cosh(rt)\end{pmatrix} \oplus \mathcal{I}_{2N-1}, \tag{24}$$

and the evolution operation $U_{\rm eig}$ is

$$U_{\rm eig} = \begin{pmatrix} e^{-i\Omega_1} & 0 \\ 0 & e^{i\Omega_1} \end{pmatrix} \bigoplus_{n\neq 1}^{2N} \begin{pmatrix} e^{-i\Omega_n} & 0 \\ 0 & e^{i\Omega_n} \end{pmatrix}. \tag{25}$$

As the unitary evolution of the DDTQW is solely Gaussian [40,41], the final state can be completely described by its covariance matrix and displacement vector (the latter being zero in this case, as there are no displacement operators). The final covariance matrix after t steps of evolution is then

$$\begin{aligned}\sigma_t &= \frac{1}{2} U_{\rm eig}^t Sq(\Gamma_F)\mathcal{I} Sq(\Gamma_F)^\dagger (U_{\rm eig}^t)^\dagger \\ &= \frac{1}{2}\begin{pmatrix} \cosh(2tr) & -e^{-2i\Omega_1 t}\sinh(2tr) \\ -e^{2i\Omega_1 t}\sinh(2tr) & \cosh(2tr) \end{pmatrix} \bigoplus \mathcal{I}_{2N-1}.\end{aligned} \tag{26}$$

The intensity in the mth mode of the squeezed DDTQW is given by $n = \langle \hat{A}_m^\dagger \hat{A}_m \rangle = \sinh^2(tr) \sim \frac{1}{2}e^{2rt}$, in the long-time t limit. Thus, in the phase-matched squeezed DDTQW, the intensity increases exponentially with time in the eigenmode m that is phase matched with the pump frequency ω.

Figure 1 shows the intensity distribution in the phase-matched squeezed DDTQW in the eigen- and physical basis, respectively, when the single-mode squeezing operator is pumped into all the $2N$ modes with pump magnitude $r = 0.1$. Pump phase ω is matched with the eigenfrequency of the first mode Ω_1. In the eigenbasis, shown in Fig. 1(a), the intensity in the phase-matched mode $m = 1$ increases exponentially with time, but in the physical basis, shown in Fig. 1(b), the intensity distributes over all the sites. Figure 2 shows the intensity distribution in the phase-mismatched squeezed DDTQW in the eigen- and physical basis, respectively, when the single-mode squeezing operator is pumped into all the $2N$ modes with pump magnitude $r = 0.1$ and the pump phase $\omega = \pi/4$. In the eigenbasis, shown in Fig. 2(a), the intensity oscillates between different eigenmodes, as well as in the physical basis, shown in Fig. 2(b).

Analysis of DDTQW using two-mode squeezing operator in eigenbasis. The second simplified case for analysis is when the two-mode squeezing operator in the eigenbasis is used to drive the walk, using Eq. (15), in the phase-matched regime.

Applying the two-mode squeezing operator on the eigenmodes $m = 1$ and $n = 2$ and using the relation (18) gives

$$\begin{aligned} &Sq_2(\Gamma_{\rm eig}) e^{-i(\Omega_1 \hat{A}_1^\dagger \hat{A}_1 + \Omega_2 \hat{A}_2^\dagger \hat{A}_2)} \\ &\quad = e^{-i(\Omega_1 \hat{A}_1^\dagger \hat{A}_1 + \Omega_2 \hat{A}_2^\dagger \hat{A}_2)} Sq_2(e^{i(\Omega_1+\Omega_2)}\Gamma_{\rm eig}), \end{aligned} \tag{27}$$

and the final squeezing operation $Sq_2(\Gamma_F)$ in the eigenbasis after t steps is

$$\begin{aligned} Sq_2(\Gamma_F) &= Sq_2(e^{i(t-1)(\Omega_1+\Omega_2)}\Gamma_{\rm eig}) \\ &\quad \times Sq_2(e^{i(\Omega_1+\Omega_2)}\Gamma_{\rm eig}) Sq_2(\Gamma_{\rm eig}). \end{aligned} \tag{28}$$

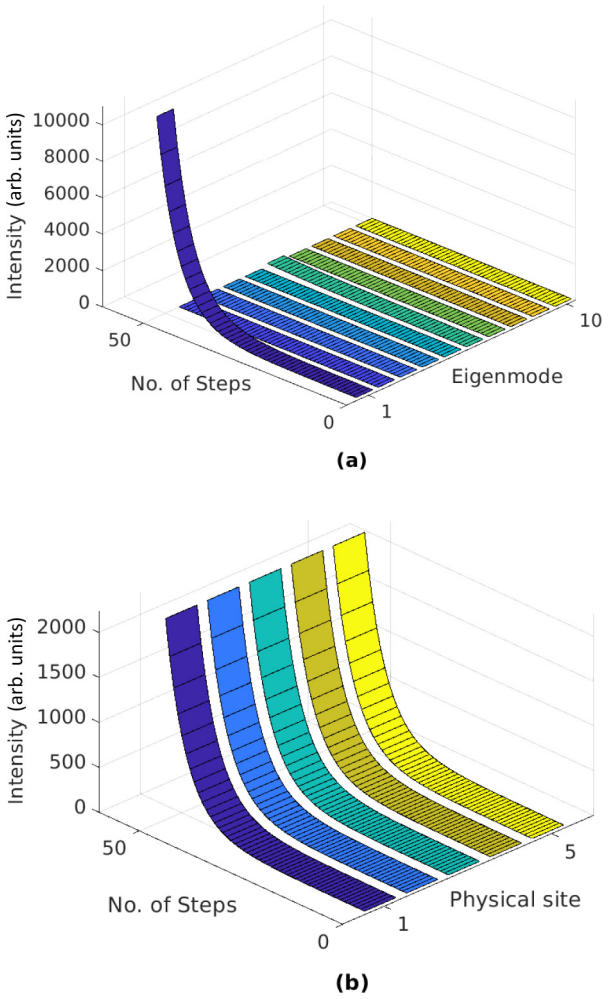

FIG. 1. Intensity distribution in phase-matched squeezed DDTQW using a single-mode squeezing operation in all $2N$ modes with respect to the number of steps, t, and phase matched with the first eigenmode in the (a) eigenbasis and (b) physical basis when the coin parameters are $(\theta, \xi, \zeta) = (\pi/4, \pi/4, 0)$ and the single-mode squeezing operation $Sq(re^{-i\omega(t-1)})$ with $r = 0.1$ and $\omega = 2\Omega_1$.

The time-dependent pump shape of the squeezing operation is given by $\Gamma_{\rm eig} = re^{-i\omega(t-1)}$ when pump phase ω is matched with the combination of eigenfrequencies $(\Omega_1 + \Omega_2)$, then,

$$Sq(\Gamma_F) = Sq(r)\cdots Sq(r)Sq(r) = [Sq(r)]^t, \tag{29}$$

which is the phase-matched condition for the two-mode squeezed DDTQW.

The symplectic form of two-mode squeezing operator $Sq_2(\Gamma_F)$ is

$$Sq_2(\Gamma_F) = \begin{pmatrix} \cosh(rt) & 0 & 0 & -\sinh(rt) \\ 0 & \cosh(rt) & -\sinh(rt) & 0 \\ 0 & -\sinh(rt) & \cosh(rt) & 0 \\ -\sinh(rt) & 0 & 0 & \cosh(rt) \end{pmatrix} \bigoplus \mathcal{I}_{2N-4}. \tag{30}$$

After t steps, the final output covariance matrix is

$$\sigma_t = \frac{1}{2} U_{\rm eig}^t Sq(\Gamma_F)\mathcal{I} Sq(\Gamma_F)^\dagger (U_{\rm eig}^t)^\dagger$$
$$= \frac{1}{2}\begin{pmatrix} \cosh(2tr) & 0 & 0 & -e^{i(\Omega_1+\Omega_2)t}\sinh(2tr) \\ 0 & \cosh(2tr) & -e^{i(\Omega_1+\Omega_2)t}\sinh(2tr) & 0 \\ 0 & -e^{-i(\Omega_1+\Omega_2)t}\sinh(2tr) & \cosh(2tr) & 0 \\ -e^{-i(\Omega_1+\Omega_2)t}\sinh(2tr) & 0 & 0 & \cosh(2tr) \end{pmatrix} \bigoplus \mathcal{I}_{2N-4}. \quad (31)$$

The intensity in the eigenmode 1 and 2 for this case is $n = \langle \hat{A}_1^\dagger \hat{A}_1 \rangle = \langle \hat{A}_2^\dagger \hat{A}_2 \rangle = \frac{1}{2}[\cosh(2rt) - 1] = \sinh^2(rt)$.

III. PHASE ESTIMATION IN DDTQW

A. Quantum parameter estimation

Quantum parameter estimation is the task to quantify the attainable measurement precision for the given quantum resources. The variance of the estimated value of an unknown parameter ξ provides a measure of this precision over all the estimation procedures. By optimizing over all the unbiased estimators and the measurements, Braunstein and Caves [58] showed that the best achievable sensitivity for measuring a small variation of the estimated parameter ξ is bounded by the quantum Cramer-Rao bound,

$$\delta\xi \geqslant \frac{1}{\sqrt{MH(\xi)}}, \quad (32)$$

where $\delta\xi$ is the error in the estimation of the unknown parameter ξ based on M measurements and $H(\xi)$ is the quantum Fisher information (QFI) for parameter ξ.

According to Refs. [59,60], the quantum Cramer-Rao bound for pure Gaussian states with displacement vector $\mathbf{d}$ and covariance matrix σ is

$$\delta\xi_{\rm min} = \frac{1}{\sqrt{M}}\left[\frac{tr[(\partial_\xi \sigma \cdot \sigma^{-1})^2]}{4} + (\partial_\xi \mathbf{d}^\dagger)\sigma^{-1}(\partial_\xi \mathbf{d})\right]^{-1/2}. \quad (33)$$

The expression in large brackets corresponds to the $H(\xi)$ for a pure multimode Gaussian state. For DDTQW driven using the squeezing operator $\mathbf{d} = 0$ with covariance matrix after evolving for t steps is σ_t (26); then the QFI $H(\xi)$ reduces to

$$H(\xi) = \frac{tr\left[\left(\partial_\xi \sigma_t \cdot \sigma_t^{-1}\right)^2\right]}{4}. \quad (34)$$

B. Analytical analysis of the phase estimation in squeezed DDTQW

In Refs. [52,53], it was shown that a quantum walker can be used for quantum metrology. In the eigenbasis, the DTQW dynamics depends upon the evolution parameters (θ, ξ), as shown in dispersion relation (12). Thus the estimation of (θ, ξ) parameters is affected by the dynamics of the walker. The QFI for the estimation of both the parameters θ and ξ encoded in the SU(2) operator, given by Eq. (1), using DTQW increases quadratically with time, i.e., as t^2.

QFI in the eigenbasis. In the following, QFI for the estimation of the phase ξ of the SU(2) operator is calculated analytically for DDTQW, using the single-mode and two-mode squeezing operators in the eigenbasis, with the phase-matched condition. The eigenbasis covariance matrix σ_t of squeezed DDTQW using a single-mode squeezing operator with the phase-matched condition in the eigenmode m after t steps is given by Eq. (26). The QFI for this case is then

$$H_{ss}(\xi) = \frac{1}{4} tr\left[\left(\partial_\xi \sigma_t . \sigma_t^{-1}\right)^2\right]$$
$$= 2t^2 (\partial_\xi \Omega_m)^2 \sinh^2(2rt). \quad (35)$$

The mean photon number for the phase-matched DDTQW using the single-mode squeezing operator is $n = \sinh^2(rt)$, meaning $H_{ss}(\xi) = 8t^2(\partial_\xi \Omega_m)^2 n(n+1)$.

The eigenbasis covariance matrix σ_t of squeezed DDTQW using the two-mode squeezing operator in the m and n eigenmodes with the phase-matched condition, after t steps, is given by Eq. (31). Thus, the QFI $H_{ts}(\xi)$ for this case is

$$H_{ts}(\xi) = \frac{1}{4} tr\left[\left(\partial_\xi \sigma_t \cdot \sigma_t^{-1}\right)^2\right]$$
$$= (\partial_\xi \Omega_m + \partial_\xi \Omega_n)^2 t^2 \sinh^2(2rt). \quad (36)$$

In terms of the mean photon number, $H_{ts} = 4(\partial_\xi \Omega_m + \partial_\xi \Omega_n)^2 t^2 n(n+1)$. In both of the cases, QFI increases as $\sinh^2(2rt)$ (exponentially in the long-time limit) with time t and pump magnitude r. If either time t or pump magnitude r is small, the QFI increases as $r^2 t^4$. The QFI in the phase-matched squeezed DDTQW also depends upon the derivative of the eigenfrequencies of the phase-matched mode.

Figure 3 shows the QFI in DDTQW using the single-mode squeezing operation in the eigenbasis. Figure 3(a) shows that the QFI increases exponentially when the squeezed DDTQW is evolved for sufficiently long time t, which is consistent with the analysis in the phase-matched regime in Sec. II B. Our analysis also shows that the QFI in the phase-matched regime of the eigenbasis depends upon the derivative of the eigenfrequency with respect to ξ, which we have plotted in Fig. 3(b). This shows the dependence of QFI with respect to $(\partial_\xi \Omega)^2$ and is maximum with respect to time when phase matched with the eigenfrequency Ω_m with the largest value of $(\partial_\xi \Omega_m)^2$.

Similarly, Fig. 4(a) shows the QFI in DDTQW using the two-mode squeezing operation in the eigenbasis, and also shows an exponential increase with time in the phase-matched regime. This condition is achieved by matching the pump frequency with the combination of eigenfrequencies of the

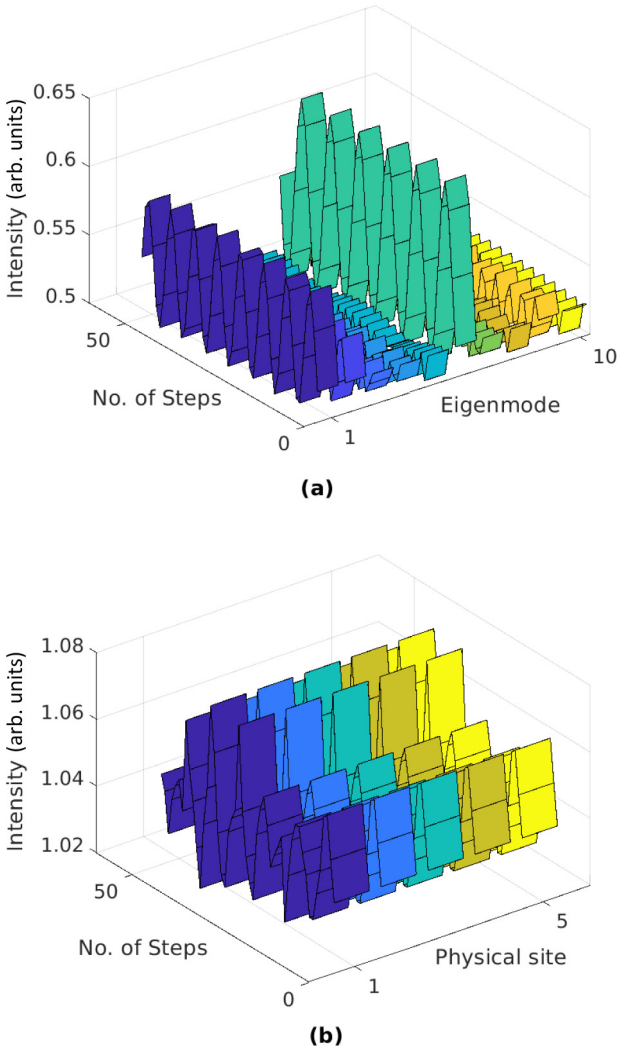

FIG. 2. Intensity distribution in phase-mismatched squeezed DDTQW using a single-mode squeezing operation in all the $2N$ modes with respect to the number of steps, t, in the (a) eigenbasis and (b) physical basis when the coin parameters are $(\theta, \xi, \zeta) = (\pi/4, \pi/4, 0)$ and the single-mode squeezing operation $Sq(re^{-i\omega(t-1)})$ with $r = 0.1$ and $\omega = \pi/4$.

two modes on which the squeezing operation is performed, i.e., if the two-mode squeezing operation is performed on the nth and the mth mode, then for the phase-matched condition, the pump frequency is $\omega = (\Omega_n + \Omega_m)$. Therefore, the QFI is maximized for the combination of eigenfrequencies for which the value of the square of $\partial_\xi(\Omega_n + \Omega_m)$ is highest. In Fig. 4(b), one can see the relation between the QFI and $\partial_\xi(\Omega_1 + \Omega_m)$ when the two-mode squeezing operator acts on the first and the m eigenmode.

QFI in the physical basis. Since the estimation protocols are performed in the physical basis, we will now examine the evolution of the QFI in that basis with time when the walk is driven using the single-mode squeezing operator in the physical mode $x = (0, \uparrow)$, i.e., $Sq_1(re^{-i\omega(t-1)})$. As the phase-matching dynamics are best analyzed in the eigenbasis, the squeezing operator must be transformed to this basis, i.e., $Sq(Re^{-i\tau(t-1)})$. This is done by rotating the pump shape to the eigenbasis, using $R = T_{\text{eig}}^{-1} r T_{\text{eig}}$, where R is a $(2N \times 2N)$ matrix. The transformation of r from the physical basis to the eigenbasis redistributes the pump shape over all $2N$ modes. After the transformation of the pump shape from the physical basis to eigenbasis, the pump frequency is matched with one of the eigenfrequencies Ω_m, i.e., $\omega = 2\Omega_m$ in Eq. (14). The DDTQW now evolves using (16). Thus, in the phase-matched regime, the QFI in the physical basis is given by

$$H_{sp}(\xi) = t^2 \sinh^2(2R_m t)(\partial_\xi \Omega_m)^2, \tag{37}$$

where R_m is the mth diagonal element of the pump shape R in the eigenbasis. This will always be less than the pump shape r in the physical basis, signifying that some pump power is lost to phase-mismatched modes.

In Fig. 5(a), we have plotted the QFI with time and pump frequency ω matched with the eigenfrequencies Ω_m in the physical basis when the single-mode squeezed state is pumped in the first physical mode, i.e., $x = (0, \uparrow)$. In Fig. 5(b), we have plotted $\Sigma^2 = [\sinh(2R_m t)\partial_\xi \Omega_m]^2$ with respect to eigenfrequencies Ω_m for $t = 50$. Figure 5(a) shows QFI with respect to time and pump-phase matched with the eigenfrequencies Ω_m such that $H_{sp}(\xi) = t^2\Sigma^2$ when evolved for 50 steps.

Due to the redistribution of r over all the $2N$ modes, QFI in the physical basis is less than QFI in the eigenbasis, which is a direct consequence of $R_m \ll r$ in Fig. 5. Thus, to achieve an equivalent improvement of QFI in the physical basis, we have studied the next interesting case where we pump the single-mode squeezed state in all the available $2N$ modes with pump magnitude r. Each of the $2N$ physical modes is pumped with the single-mode squeezing operator $Sq_1(\Gamma_m) = Sq_1(re^{-i\omega(t-1)})$, such that the final squeezing operator $Sq(r'e^{-i\omega'(t-1)})$ is given by

$$Sq(r'e^{-i\omega'(t-1)}) = \prod_{m=1}^{2N} Sq_1(\Gamma_m) = Sq(re^{-i\omega(t-1)}\mathcal{I}_{2N}), \tag{38}$$

where $r' = r\mathcal{I}_{2N}$ and $e^{-i\omega'(t-1)} = e^{-i\omega(t-1)}\mathcal{I}_{2N}$ are the pump magnitude and pump phase, respectively, and $\mathcal{I}_{2N}$ is the identity matrix of size $2N$. In this case, the pump magnitude R of the $2N$-mode squeezing operation remains under the basis transformation from physical basis to eigenbasis since $Re^{i\tau(t-1)} = T_{\text{eig}}^{-1} r' e^{-i\omega'(t-1)} T_{\text{eig}} \equiv re^{-i\omega(t-1)}\mathcal{I}_{2N}$. The QFI, in both the physical basis and the eigenbasis, is equal to $[t \sinh(2rt)\partial_\xi(\Omega_m)]^2$. Figure 6 shows comparable QFI in both bases with respect to time and eigenfrequencies in the phase-matched regime.

QFI in the phase-mismatched regime. In the phase-mismatched regime of the squeezed DDTQW, numerical simulations show that QFI is proportional to $[t \sinh(r)]^2$, implying that the increase in QFI in the phase-mismatched squeezed DDTQW is comparable to the QFI in DTQW as in both the cases the QFI increases quadratically with time t.

In the physical basis, QFI is proportional to $[t \sinh(R_m)]^2$, where R_m is the same as explained for Eq. (37). Figure 7 shows the QFI in this regime with respect to time and ξ in the physical basis, and it is independent of the parameter ξ to be estimated. Figure 8 shows QFI in the phase-mismatched regime with respect to the number of steps, t, for different

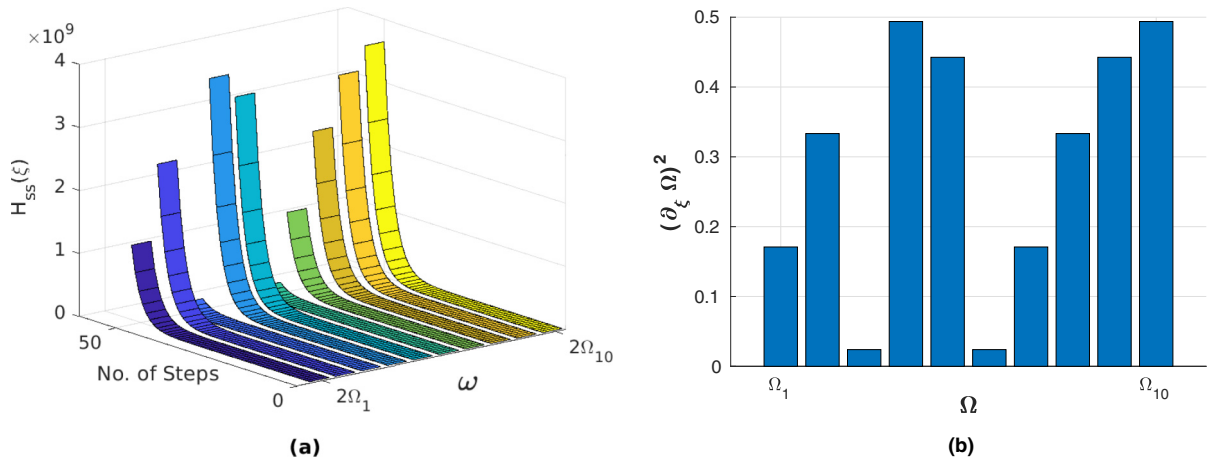

FIG. 3. QFI in squeezed DDTQW using the single-mode squeezing operation in the eigenbasis. (a) $H_{ss}(\xi)$ in the eigenbasis with number of steps, t, and pump phase ω, phase matched with twice the eigenfrequency Ω_m. (b) Square of the derivative of eigenfrequencies Ω_m. Here, the pump magnitude is $r = 0.1$ and the evolution parameters are $(\theta, \xi, \zeta) = (\pi/4, \pi/4, 0)$, and the single-mode squeezed state is pumped in the mode $m \in [1, 10]$.

values of pump magnitude r, which shows that QFI increases with the increase in pump magnitude r.

C. Comparison with previous approaches

According to the quantum Cramer-Rao bound, the variance of an estimated parameter ξ is

$$(\delta\xi)^2 \geqslant \frac{1}{MH(\xi)}, \tag{39}$$

where M is the number of measurements and $H(\xi)$ is the QFI for the estimated parameter. Therefore, the variance in DDTQW is bounded by the inverse of Eqs. (35) and (36), which are the QFI for phase-matched DDTQW using single-mode and two-mode squeezed states, respectively. Thus, the minimum variance in DDTQW for both cases is proportional to $1/[t^2 n(n+1)]$. We now compare our method of phase estimation with two previous methods, i.e., the original DTQW and the SU(1,1) interferometer.

First, for the standard DTQW, given by Eq. (3) in Ref. [53], the QFI scales as $O(t^2)$, as this method uses a single particle throughout the walk. It is therefore immediate to see that the QFI is increased in the DDTQW by the extra photons that are present. To compensate for this using the DTQW, there could either be $M = O(n^2)$ repeated applications of the protocol or more photons added in the initial state.

Another important comparison is with the SU(1,1) interferometer, which can be considered as a single time step of the DDTQW. SU(1,1) interferometers are nonlinear devices that use optical parametric amplifiers instead of beam splitters [61] in a Mach-Zehnder-like configuration. Reference [54] shows that the QFI in the SU(1,1) interferometer is $4n(n+2)$, where n is the average number of photons, which is lower than the DDTQW by a factor of t^2. However, as the dynamics of the DDTQW involves t time steps with $2t$ modes, a better

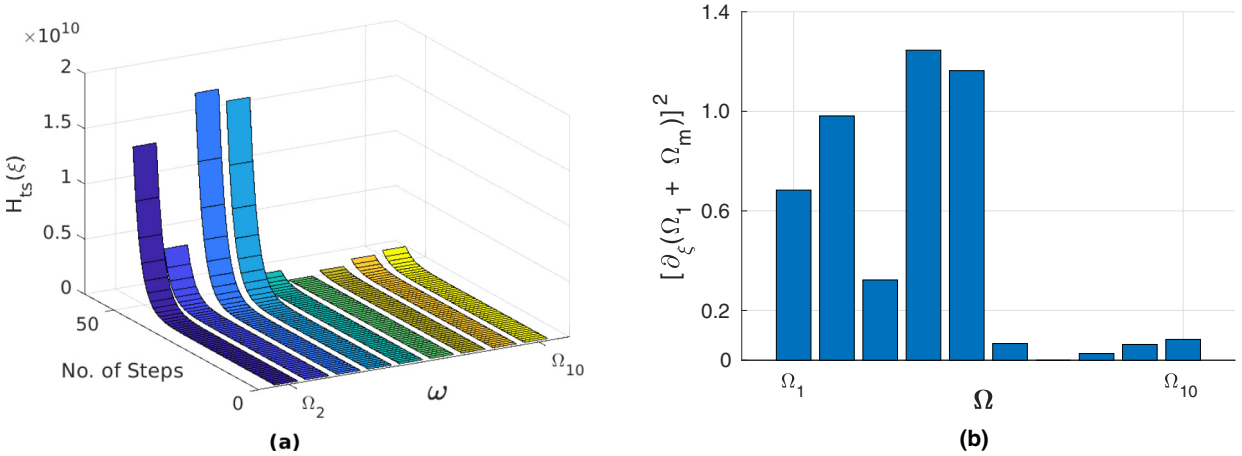

FIG. 4. QFI in squeezed DDTQW using two-mode squeezing operation in the eigenbasis. (a) $H_{ts}(\xi)$ in the eigenbasis with number of steps, t, and the pump phase ω, phase matched with the combination of eigenfrequencies $(\Omega_1 + \Omega_m)$, where mode $m \in [2, 10]$. (b) Value of the square of $\partial_\xi(\Omega_1 + \Omega_m)$. Here, pump magnitude $r = 0.1$, the evolution parameters are $(\theta, \xi, \zeta) = (\pi/4, \pi/4, 0)$, and two-mode squeezed state is pumped into modes 1 and $m \in [2, 10]$.

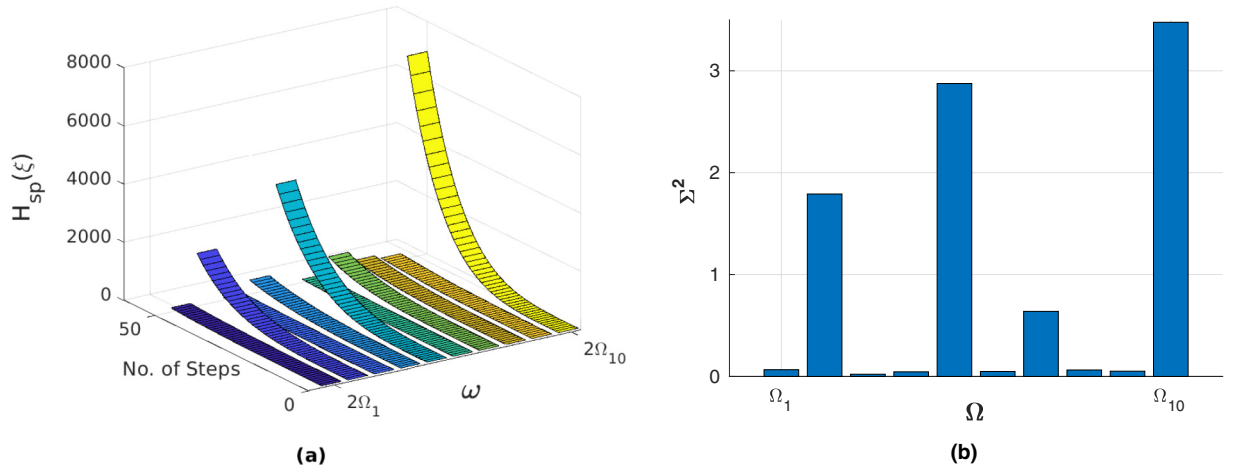

FIG. 5. QFI in squeezed DDTQW using the single-mode squeezing operation in the physical basis when pumped in the mode $(x = 0, \uparrow)$. (a) $H_{sp}(\xi)$ in the physical basis with number of steps, t, and pump frequency ω, matched with twice the eigenfrequency Ω_m. (b) Value of the square of $\Sigma = (\partial_\xi \Omega_m)\sinh(2tR_m)$, where R_m is the diagonal element of the transformed magnitude r from the physical basis to the eigenbasis. Here, pump magnitude in the physical basis is $r = 0.1$ for the single-mode squeezing operator and the evolution parameters are $(\theta, \xi, \zeta) = (\pi/4, \pi/4, 0)$ when pumped in the modes $1 \equiv (x = 0, \uparrow)$.

comparison is with t repeated applications of the SU(1,1) interferometer. This would only result in a factor of $1/t$ in the variance, not $1/t^2$ as in the DDTQW. This increase in the QFI has been attributed to the presence of entanglement between the different modes of the total system [62,63], something not present in repeated uses of the SU(1,1) interferometer.

IV. EIGENFREQUENCY ANALYSIS TO ACHIEVE MAXIMUM QFI

The eigenfrequency of the unitary evolution operator U (11) plays a vital role in achieving the exponential increase of the QFI in the squeezed-DDTQW dynamics. Therefore, an analysis of the eigenfrequencies' dependence upon the evolution parameter will give crucial information on the choice of the pump frequency to achieve the phase-matched condition.

In general, it does not matter which eigenfrequency is phase matched, as they all allow for exponential scaling when evolved for a sufficiently long time. To be precise, the QFI for ξ is proportional to the square of the derivative of the eigenfrequency Ω_m with respect to ξ,

$$(\partial_\xi \Omega_m)^2 = \frac{[\cos^2(\theta) - \cos^2(\Omega_m)]}{\sin^2(\Omega_m)}. \tag{40}$$

From the dispersion relation, given by Eq. (12), it can be shown that Ω_m is always greater than θ and thus always gives a positive value of $(\partial_\xi \Omega_m)^2$. The magnitude of smallest eigenfrequency, $|\Omega_{\min}|$, is lower bounded by the parameter θ. This can be shown by a simple analysis of the dispersion relation, given by Eq. (12), of the quantum walker in DTQW. The maximum value of the $\cos(\xi - 2\pi k_0/N)$ term in the dispersion relation, given by Eq. (12), is 1, implying that corresponding

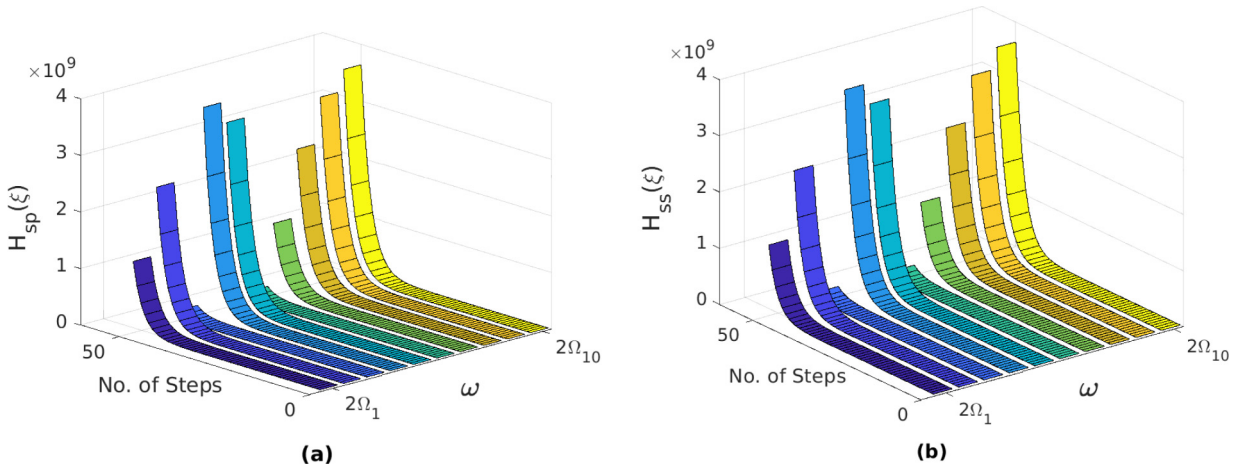

FIG. 6. QFI in squeezed DDTQW using the single-mode squeezing operation in all the available $2N$ modes in the physical basis. (a) H_{sp} in the physical basis and (b) H_{ss} in the eigenbasis, with respect to the number of steps, t, and the pump phase ω when phase matched with twice the eigenfrequency Ω_m. Here, all the available $2N$ modes are pumped with the squeezing operator with same pump magnitude $r = 0.1$ and the evolution parameters are $(\theta, \xi, \zeta) = (\pi/4, \pi/4, 0)$.

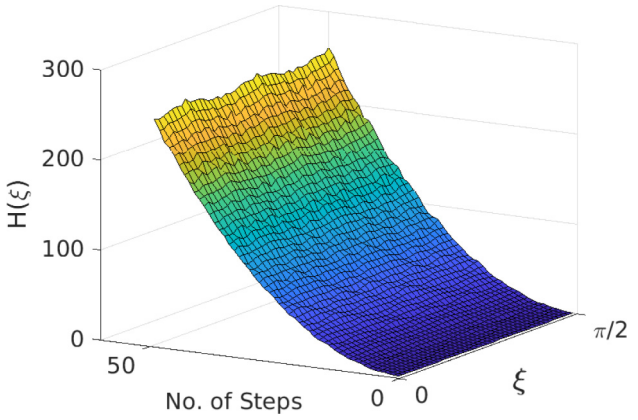

FIG. 7. QFI in phase-mismatched squeezed DDTQW using the single-mode squeezing operation in all the available $2N$ modes in the physical basis with respect to t steps and parameter ξ. Here, all the $2N$ modes are pumped with the squeezing operator with magnitude $r = 0.1$ and pump phase $\omega = \pi/4$. The evolution parameters are $(\theta, \zeta) = (\pi/4, 0)$ and evolved for $t = 50$ steps.

to k_0,

$$\cos(\Omega_{k_0}) \leqslant \cos(\theta),$$
$$\Omega_{k_0} \geqslant \theta, \tag{41}$$

i.e., the eigenfrequency Ω_{k_0} is lower bounded by $\theta \in [0, \pi/2]$. The pump frequency $\omega = 2\Omega_m$ for phase-matched DDTQW, as shown in Eq. (22), gives a lower bound over the pump phase in terms of the θ parameter as

$$\omega \geqslant 2\theta, \tag{42}$$

for $\omega \in [0, \pi]$. Figure 9 shows QFI with respect to pump phase ω and coin parameter θ. It can be seen from the plot that enhanced QFI with respect to pump phase ω is bounded by θ. The enhancement of the QFI is seen on the graph for $\omega > 2\theta$.

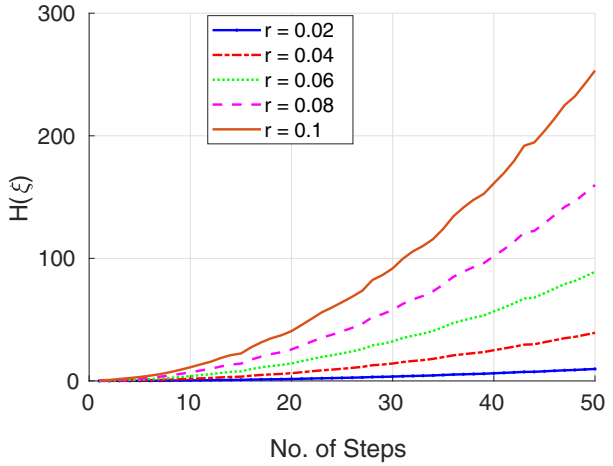

FIG. 8. QFI in phase-mismatched squeezed DDTQW using the physical-basis single-mode squeezing operation in all $2N$ modes, with respect to the number of steps for different values of pump magnitude r. The evolution parameters are $(\theta, \xi, \zeta) = (\pi/4, \pi/4, 0)$ and pump phase $\omega = \pi/4$.

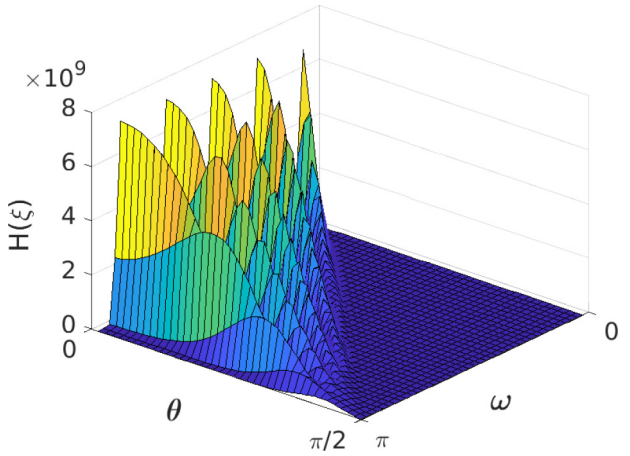

FIG. 9. QFI in squeezed DDTQW using single-mode squeezing operation in all the $2N$ modes in the physical basis with respect to parameter θ and pump phase ω. Here, $2N$ modes are pumped with the squeezing operator with pump magnitude $r = 0.1$ and pump phase $\omega = \pi/4$. The evolution parameters are $(\theta, \zeta) = (\pi/4, 0)$ evolved for $t = 50$.

V. CONCLUSION

In this work, we have investigated a method for quantum enhanced precision in the estimation of the phase ξ encoded in the evolution operator of the quantum walker using DDTQW, a different type of QW that includes the effect of walker creation and destruction throughout the walk. We have analytically calculated the QFI in DDTQW using the squeezing operator on a cyclic graph of N sites. Our numerical studies show that in the phase-mismatched case, the QFI, $H(\xi) \propto t^2$, which is comparable to the phase estimation in DTQW [53]. When the DDTQW operates in the phase-matched regime, the enhancement in the QFI can be r^2t^4 for small rt and exponential for $rt \gg 1$, where the squeezing parameter is r.

The reason for enhanced $H(\xi)$ in the phase-matched case can be attributed to the constructive interference between the walkers (photons) in the phase-matched eigenmode that lead to an exponential increase in the intensity with time in that eigenmode. We have compared the phase estimation using DDTQW with the standard DTQW and the SU(1,1) interferometer. We also provide a bound over the pump frequency to achieve phase-matched DDTQW in the estimation of ξ with enhanced precision. In the phase-matched DDTQW, the pump frequency ω is always greater than 2θ when $\theta \in [0, \pi/2]$.

In this work, we have introduced a way to enhance the quantum precision of phase estimation in QW dynamics using a driving term. The work here using DDTQW can be further developed for quantum metrological tasks by adding measurements and feedforward, improving the sensitivity in an estimation protocol with the help of the driving operator.

ACKNOWLEDGMENTS

The authors acknowledge the financial support from RVO14000 and "Centre for Advanced Applied Sciences," Registry No. CZ.02.1.01/0.0/0.0/16019/0000778, supported

by the Operational Programme Research, Development and Education, co-financed by the European Structural and Investment Funds. I.J. is grateful for the financial support from GAČR of the Czech Republic under Grant No. 23-07169S.

[1] S. Venegas-Andraca, Quantum walks: A comprehensive review, Quantum Inf. Proc. **11**, 1015 (2012).
[2] D. Reitzner, D. Nagaj, V. Buzek, Quantum walks, arXiv:1207.7283.
[3] J. Kempe, Quantum random walks: An introductory overview, Contemp. Phys. **44**, 307 (2003).
[4] A. M. Childs, Universal computation by quantum walk, Phys. Rev. Lett. **102**, 180501 (2009).
[5] N. B. Lovett, S. Cooper, M. Everitt, M. Trevers, and V. Kendon, Universal quantum computation using the discrete time quantum walk, Phys. Rev. A **81**, 042330 (2010).
[6] S. Singh, P. Chawla, A. Sarkar, and C. M. Chandrashekar, Universal quantum computing using single-particle discrete-time quantum walk, Sci. Rep. **11**, 11551 (2021).
[7] R. Portugal, *Quantum Walks and Search Algorithms*, Vol. 19 (Springer, New York, 2013).
[8] F. Magniez, A. Nayak, J. Roland, and M. Santha, Search via quantum walk, SIAM J Sci Comput. **40**, 142 (2011).
[9] M. Mohseni, P. Rebentrost, S. Lloyd and A. Aspuru-Guzik, Environment-assisted quantum walks in photosynthetic energy transfer, J. Chem. Phys. **129**, 174106 (2008).
[10] A. Schreiber, K. N. Cassemiro, V. Potoček, A. Gábris, I. Jex, and Ch. Silberhorn, Decoherence and disorder in quantum walks: From ballistic spread to localization, Phys. Rev. Lett. **106**, 180403 (2011).
[11] A. Joye, and M. Merkli, Dynamical localization of quantum walks in random environments, J. Stat. Phys. **140**, 1025 (2010).
[12] P. Törmä, I. Jex, and W. P. Schleich, Localization and diffusion in Ising-type quantum networks, Phys. Rev. A **65**, 052110 (2002).
[13] D. A. Mayer, From quantum cellular automata to quantum lattice gases, J. Stat. Phys. **85**, 551 (1996).
[14] A. Mallick and C. M. Chandrashekar, Dirac cellular automaton from split-step quantum walk, Sci. Rep. **6**, 25779 (2016).
[15] I. Bialynicki-Birula, Weyl, Dirac, and Maxwell equations on a lattice as unitary cellular automata, Phys. Rev. D **49**, 6920 (1994).
[16] G. Di Molfetta, and A. Pérez, Quantum walks as simulators of neutrino oscillations in a vacuum and matter, New J. Phys. **18**, 103038 (2016).
[17] T. Kitagawa, M. Rudner, E. Berg, and E. Demler, Exploring Topological Phases with quantum walk, Phys. Rev. A **82**, 033429 (2010).
[18] A. P. Schnyder, S. Ryu, A. Furusaki, and A. W. W. Ludwig, Classification of topological insulators and superconductors in three spatial dimensions, Phys. Rev. B **78**, 195125 (2008).
[19] J. K. Asboth and H. Obuse, Bulk-boundary correspondence for chiral symmetric quantum walks, Phys. Rev. B **88**, 121406(R) (2013).
[20] T. Oka, N. Konno, R. Arita, and H. Aoki, Breakdown of an electric-field driven system: A mapping to a quantum walk, Phys. Rev. Lett. **94**, 100602 (2005).
[21] S. Godoy and S. Fujita, A quantum random-walk model for tunneling diffusion in a 1D lattice, A quantum correction to Fick's law, J. Chem. Phys. **97**, 5148 (1992).
[22] C. A. Ryan, M. Laforest, J.-C. Boileau, and R. Laflamme, Experimental implementation of a discrete-time quantum random walk on an NMR quantum-information processor, Phys. Rev. A **72**, 062317 (2005).
[23] A. Schreiber, K. N. Cassemiro, V. Potocek, A. Gabris, P. J. Mosley, E. Andersson, I. Jex, and C. Silberhorn, Photons walking the line: A quantum walk with adjustable coin operations, Phys. Rev. Lett. **104**, 050502 (2010).
[24] M. A. Broome, A. Fedrizzi, B. P. Lanyon, I. Kassal, A. Aspuru-Guzik, and A. G. White, Discrete single-photon quantum walks with tunable decoherence, Phys. Rev. Lett. **104**, 153602 (2010).
[25] M. Karski, L. Forster, J.-M. Choi, A. Steffen, W. Alt, D. Meschede, and A. Widera, Quantum walk in position space with single optically trapped atoms, Science **325**, 174 (2009).
[26] H. Schmitz, R. Matjeschk, C. Schneider, J. Glueckert, M. Enderlein, T. Huber, and T. Schaetz, Quantum walk of a trapped ion in phase space, Phys. Rev. Lett. **103**, 090504 (2009).
[27] F. Zähringer, G. Kirchmair, R. Gerritsma, E. Solano, R. Blatt, and C. Roos, Realization of a quantum walk with one and two trapped ions, Phys. Rev. Lett. **104**, 100503 (2010).
[28] C. Huerta Alderete, S. Singh, N. H. Nguyen, D. Zhu, R. Balu, C. Monroe, C. M. Chandrashekar and N. M. Linke, Quantum walks and Dirac cellular automata on a programmable trapped-ion quantum computer, Nat. Commun. **11**, 3720 (2020).
[29] A. Peruzzo, M. Lobino, J. C. Matthews, N. Matsuda, A. Politi, K. Poulios, X.-Q. Zhou, Y. Lahini, N. Ismail, K. Worhoff *et al.*, Quantum walks of correlated photons, Science **329**, 1500 (2010).
[30] H. B. Perets, Y. Lahini, F. Pozzi, M. Sorel, R. Morandotti, and Y. Silberberg, Realization of quantum walks with negligible decoherence in waveguide lattices, Phys. Rev. Lett. **100**, 170506 (2008).
[31] G. V. Riazanov, The Feynman path integral for the Dirae equation, J. Exptl. Theoret. Phys. (U.S.S.R.) **33**, 1437 (1957) [Sov. Phys. JETP **6**, 1107 (1958)].
[32] R. P. Feynman, Quantum mechanical computers, Found. Phys. **16**, 507 (1986).
[33] Y. Aharonov, L. Davidovich, and N. Zagury, Quantum random walks, Phys. Rev. A **48**, 1687 (1993).
[34] A. Nayak and A. Vishwanath, Quantum walk on the line, arXiv:quant-ph/0010117.
[35] N. Inui, N. Konno, and E. Segawa, One-dimensional three-state quantum walk, Phys. Rev. E **72**, 056112 (2005).
[36] D. Solenov, and L. Fedichkin, Continuous-time quantum walks on a cycle graph, Phys. Rev. A **73**, 012313 (2006).
[37] A. M. Childs, On the Relationship Between Continuous- and Discrete-Time Quantum Walk, Commun. Math. Phys. **294**, 581 (2010).

[38] N. Konno, Limit theorem for continuous-time quantum walk on the line, Phys. Rev. E **72**, 026113 (2005).
[39] C. M. Chandrashekar, R. Srikanth, and R. Laflamme, Optimizing the discrete time quantum walk using a SU(2) coin, Phys. Rev. A **82**, 019902(E) (2010).
[40] C. S. Hamilton, R. Kruse, L. Sansoni, C. Silberhorn, and I. Jex, Driven quantum walks, Phys. Rev. Lett. **113**, 083602 (2014).
[41] C. S. Hamilton, S. Barkhofen, L. Sansoni, I. Jex, and C. Silberhorn. Driven discrete time quantum walks, New J. Phys. **18**, 073008 (2016).
[42] R. Kruse, F. Katzschmann, A. Christ, A. Schreiber, S. Wilhelm, K. Laiho, A. Gábris, C. S. Hamilton, I. Jex and C. Silberhorn, Spatio-spectral characteristics of parametric down-conversion in waveguide arrays, New J. Phys. **15**, 083046 (2013).
[43] A. Solntsev, F. Setzpfandt, A. Clark, C. W. Wu, M. Collins, C. Xiong, A. Schreiber, F. Katzschmann, F. Eilenberger, R. Schiek, W. Sohler, A. Mitchell, C. Silberhorn, B. Eggleton, T. Pertsch, A. Sukhorukov, D. Neshev, and Y. Kivshar, Generation of nonclassical biphoton states through cascaded quantum walks on a nonlinear chip, Phys. Rev. X **4**, 031007 (2014).
[44] A. Regensburger, C. Bersch, B. Hinrichs, G. Onishchukov, A. Schreiber, C. Silberhorn and U. Peschel, Photon propagation in a discrete fiber network: An interplay of coherence and losses, Phys. Rev. Lett. **107**, 233902 (2011).
[45] The LIGO Scientific Collaboration, A gravitational wave observatory operating beyond the quantum shot-noise limit, Nat. Phys. **7**, 962 (2011).
[46] A. Shabani, M. Mohseni, S. Lloyd, R. L. Kosut, and H. Rabitz, Estimation of many-body quantum Hamiltonians via compressive sensing, Phys. Rev. A **84**, 012107 (2011).
[47] C. Degen, F. Reinhard, and P. Cappellaro, Quantum sensing, Rev. Mod. Phys. **89**, 035002 (2017).
[48] E. Polino, M. Valeri, N. Spagnolo, and F. Sciarrino, Photonic quantum metrology, AVS Quantum Sci. **2**, 024703 (2020).
[49] C. Helstrom, Quantum detection and estimation theory, J. Stat. Phys. **1**, 231 (1969).
[50] M. Hillery, J. Bergou, and E. Feldman, Quantum walks based on an interferometric analogy, Phys. Rev. A **68**, 032314 (2003).
[51] F. Zatelli, C. Benedetti, and M. G. Paris, Scattering as a quantum metrology problem: A quantum walk approach, Entropy **22**, 1321 (2020).
[52] S. Singh, C. M. Chandrashekar, and M. G. Paris, Quantum walker as a probe for its coin parameter, Phys. Rev. A **99**, 052117 (2019).
[53] M. Annabestani, M. Hassani, D. Tamascelli, and M. G. Paris, Multiparameter quantum metrology with discrete-time quantum walks, Phys. Rev. A **105**, 062411 (2022).
[54] J. Qin, Y. Deng, H. Zhong, L. Peng, H. Su, Y. Luo, J. Xu, D. Wu, S. Gong, H. Liu, H. Wang, M. Chen, L. Li, N. Liu, C. Lu, and J. Pan, Unconditional and robust quantum metrological advantage beyond noon states, Phys. Rev. Lett. **130**, 070801 (2023)
[55] I. Vakulchyk, M. V. Fistul, P. Qin, and S. Flach, Anderson localization in generalized discrete-time quantum walks, Phys. Rev. B **96**, 144204 (2017).
[56] S. Barnett, and P. Radmore, Methods in Theoretical Quantum Optics (Oxford University Press, Oxford, 2002).
[57] D. Šafránek, A. Lee and I. Fuentes, Quantum parameter estimation using multi-mode Gaussian states, New J. Phys. **17**, 073016 (2015).
[58] S. L. Braunstein and C. M. Caves, Statistical distance and the geometry of quantum states, Phys. Rev. Lett. **72**, 3439 (1994).
[59] O. Pinel, J. Fade, D. Braun, P. Jian, N. Treps, and C. Fabre, Ultimate sensitivity of precision measurements with intense Gaussian quantum light: A multimodal approach, Phys. Rev. A **85**, 010101(R) (2012).
[60] A. Monras, Phase space formalism for quantum estimation of Gaussian states, arXiv:1303.3682.
[61] B. Yurke, S. L. McCall, and J. R. Klauder, SU(2) and SU(1, 1) interferometers, Phys. Rev. A **33**, 4033 (1986).
[62] M. Oszmaniec, R. Augusiak, C. Gogolin, J. Kołodyński, A. Acín, and M. Lewenstein, Random bosonic states for robust quantum metrology, Phys. Rev. X **6**, 041044 (2016).
[63] H. Kwon, Y. Lim, L. Jiang, H. Jeong, and C. Oh, Quantum metrological power of continuous-variable quantum networks, Phys. Rev. Lett. **128**, 180503 (2022).